Journal of Nuclear Medicine, published on January 19, 2023 as doi:10.2967/jnumed.122.264594

Towards Single Time Point Image-Based Dosimetry of ^{177}Lu-PSMA-617 Therapy

Julia Brosch-Lenz[1,2,*], Astrid Delker[1], Friederike Völter[1], Lena M. Unterrainer[1], Lena Kaiser[1], Peter Bartenstein[1], Sibylle Ziegler[1], Arman Rahmim[2,3,4], Carlos Uribe[3,5], Guido Böning[1]

[1]Department of Nuclear Medicine, University Hospital, LMU Munich, Munich, Germany

[2]Department of Integrative Oncology, BC Cancer Research Institute, Vancouver, BC, Canada

[3]Department of Radiology, University of British Columbia, Vancouver, BC, Canada

[4]Department of Physics, University of British Columbia, Vancouver, BC, Canada

[5]Department of Functional Imaging, BC Cancer, Vancouver, BC, Canada

***Correspondence should be addressed to**

Julia Brosch-Lenz

Post-Doctoral Fellow

Julia.Brosch-Lenz@med.uni-muenchen.de; jbrosch@bccrc.ca

Department of Integrative Oncology, BC Cancer Research Centre, 675 West 10th Avenue, Vancouver, BC, V5Z 1L3, Canada

Short title: ^{177}Lu-PSMA Single Time Point Dosimetry

Keywords: Single Time Point Dosimetry; Lutetium-177; PSMA therapy

Word count: 5525

ABSTRACT

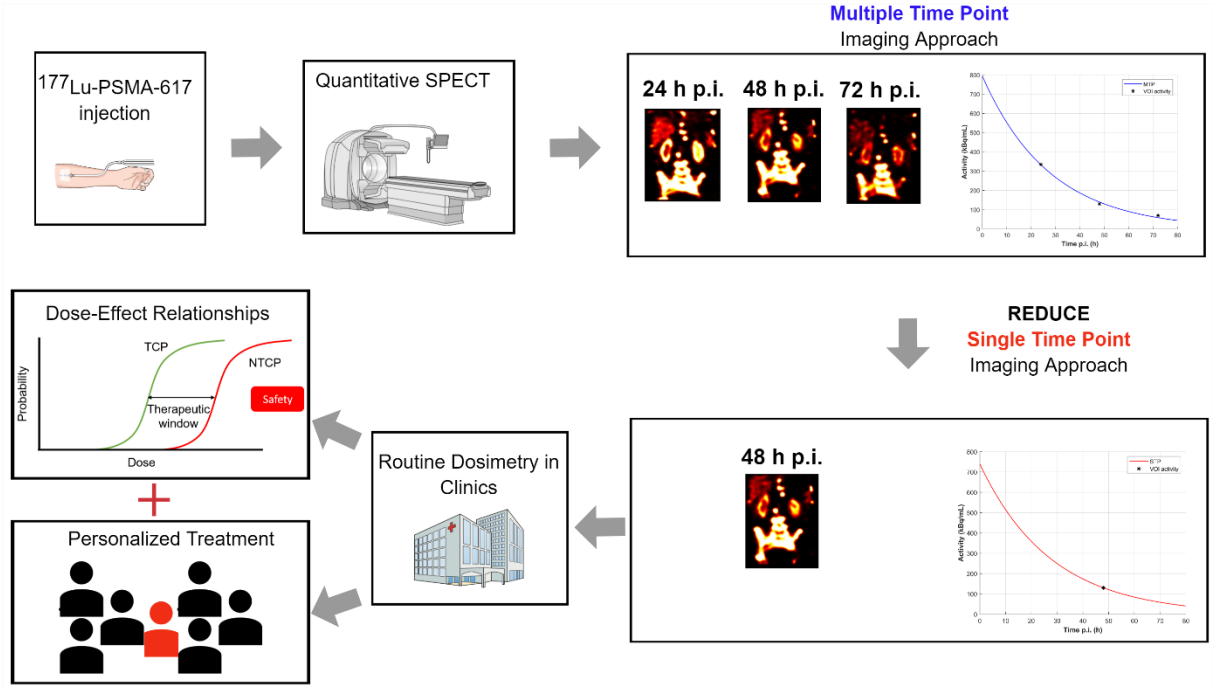

Radiopharmaceutical therapies (RPTs) with Lutetium-177 prostate-specific membrane antigen (PSMA) ligands have demonstrated promising results for the treatment of metastatic castration-resistant prostate cancer (mCRPC). The lack of absorbed dose and effect relationships currently prevents from patient-specific activity personalization. To ease the implementation of dosimetry in routine clinic workflow of RPT, simplified methods such as single time point (STP) instead of multiple time point (MTP) imaging protocols are required. This work aims at assessing differences in time-integrated activity (TIA) of STP versus MTP image-based dosimetry for ^{177}Lu-PSMA-617 therapy. **Methods:** 20 mCRPC patients with MTP quantitative ^{177}Lu-SPECT imaging data (~24h, 48h, 72h post administration) available on first and second ^{177}Lu-PSMA-617 therapy cycles were included in this study. Time-activity-curves were fitted for kidneys and lesions to derive effective half-lives and yield reference TIA. STP approaches involved the formula by Hänscheid (STP_H) and a prior information method (STP_{prior}) that uses the effective half-lives from the first therapy cycle. All time points were considered for the STP approaches. Percentage differences (PD) in TIA between STP and MTP was compared for the second therapy cycle. **Results:** Using STP_H at 48h p.i. for the kidneys had -1.3±5.6% difference against MTP, while STP_{prior} showed a PD of 4.6±6.2%. Smallest average

differences for the 56 investigated individual lesions were found using the STP_{prior} approach at 48h p.i. with only 0.4±14.9%, while STP_H at 72h p.i. had smallest PD of -1.9±14.8%. **Conclusion:** STP dosimetry for ^{177}Lu-PSMA-617 therapy using a single SPECT/CT at 48h or 72h is feasible with a difference of <±20% compared against MTP. Both, STP_H and STP_{prior} have demonstrated their validity. We believe this finding can increase the adoption of dosimetry and facilitate implementation in routine clinical RPT workflows. Doing so will ultimately enable the finding of dose-effective relationships based on fixed therapy activities that could in future allow for absorbed dose based RPT activity personalization.

INTRODUCTION

Radiopharmaceutical therapy (RPT) targeting the prostate-specific membrane antigen (PSMA) has shown significant promise in the treatment of metastatic, castration-resistant prostate cancer (mCRPC) (*1*-*3*). PSMA radioligand therapy with Lutetium-177 (^{177}Lu) was first conducted in 2013 (*4*), and shortly after, dosimetry results were reported for ^{177}Lu-PSMA-617 (*5*). Considerable improvements in overall survival and radiographic progression-free survival, for mCRPC patients receiving ^{177}Lu-PSMA-617 therapy plus standard of care against standard of care alone in the VISION trial (NCT03511664) (*1*) led to approval by the US Food and Drug Administration agency in 2022. Although some evidence of the advantage of dosimetry-based treatment personalization has been shown recently for Yttrium-90 liver radioembolization (*6*), current practice for most RPTs rely on fixed injected activities. The therapeutic scheme for ^{177}Lu-PSMA therapy involves four to six therapy cycles with fixed activities (*7*) while optimal patient treatment would consider individual factors such as weight, height, tumor burden, pre-treatments, dosimetry and patients' preferences during RPT planning (*8*). The lack of broadly available absorbed doses (ADs) for RPT prevent from obtaining reliable dose-effect relationships for lesions and healthy organs impeding treatment personalization in terms of activity and number of therapy cycles (*9*). The possibility to correlate pre-therapy information with dosimetry and patient outcome was recently shown (*10*) and should further motivate the community to implement routine dosimetry within the RPTs and actively plan and adapt RPT to personalize treatment and maximize patient therapeutic benefit.

The evidence of patient benefit from personalized RPTs is currently limited by the fact that image-based dosimetry is still not routinely implemented along with RPTs. One of the limitations for clinically adoption of patient-individual dosimetry is that the measurement of the pharmacokinetics typically requires image acquisitions at multiple time points (MTP) post injection (p.i.) of the radiopharmaceutical. Other factors such as limited clinical resources (e.g. scanner availability and personnel) as well as the additional costs of MTP imaging with unclear reimbursement (*11*) limit the application of personalized

dose assessments. This however, goes against the European council directive 2013/79/Euratom that requests for individual planning and verification of exposed target volumes, and to minimize dose to non-target regions according to the ALARA principle (*12*).

In this work, we aimed to assess single time point (STP) image-based dosimetry of ^{177}Lu-PSMA-617 therapy for the second therapy cycle. Specifically, we considered the formula by Hänscheid et al. (*13*) and a prior information STP approach that uses MTP imaging during the first therapy cycle and STP imaging for subsequent cycles. We believe that validation of a simple dosimetry approach that requires a single SPECT/CT scan can increase the adoption of dosimetry and facilitate implementation in routine clinical RPT workflows. Doing so can enable the finding of dose-response relationships based on fixed therapy activities that will ultimately allow for AD based RPT activity personalization.

MATERIAL AND METHODS

Patients

This study was conducted on a cohort of patients with mCRPC that received two cycles of ^{177}Lu-PSMA-617 of 6GBq. 20 patients with MTP imaging data available on both of their therapy cycles were included in this study. Therapeutic injections and subsequent imaging were performed at the department of nuclear medicine of the university hospital of the LMU Munich, Germany. The data was irreversibly anonymized. The institutional ethics committee approved this retrospective study and the requirement to obtain informed consent was waived (Ethics Committee of LMU Munich 21-0618).

Imaging Protocol

The details of the MTP imaging protocol (Figure 1) can be found in the supplementary data (*5,14-17*).

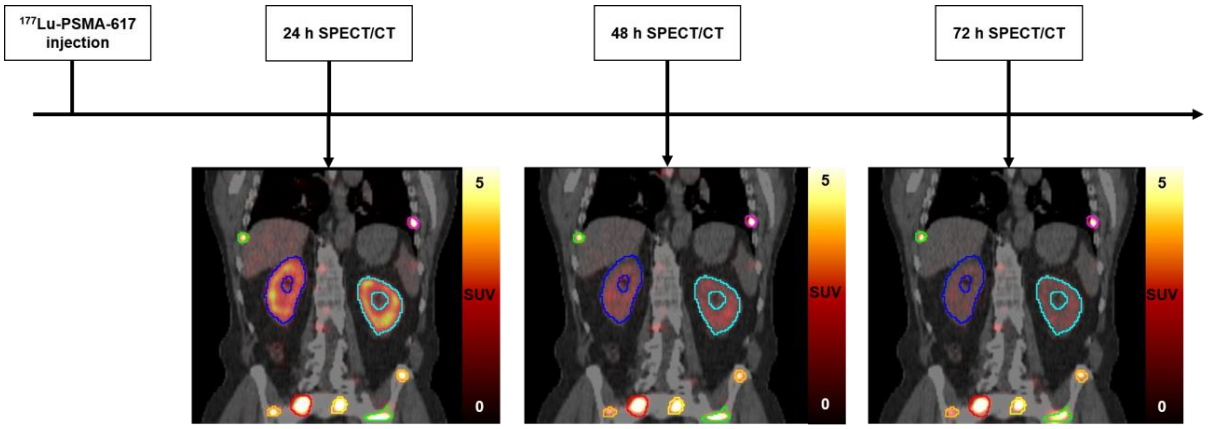

Figure 1: *Overview of MTP imaging protocol.*

Determination of Time-Activity Curves

Image processing was performed using PMOD (v4.005; PMOD Technologies LLC). The 24h SPECT of each therapy cycle was chosen as reference image to which the 48h and 72h SPECTs were rigidly registered. Segmentation was performed on the 24h SPECT scans of each cycle. Kidneys were segmented by applying a 20% fixed threshold, which was observed to produce a good alignment when overlaying the kidney volumes of interest (VOIs) on the CT, excluding the kidney pelvis. Manual adjustments were made when necessary. The qPSMA approach of Gafita et al. (*18*) was adopted for segmentation of individual lesions on the 24h SPECT per cycle, which was converted into standardized uptake values (SUV) based on body-weight. The so determined patient- and cycle-specific threshold was applied to the 24h SUV SPECT with an automatic multi-region approach. Physiological uptake regions that were mistakenly selected as VOIs by the automatic multi-region threshold approach, e.g. in the gastrointestinal tract or in the bladder, were removed. Lastly, a whole field-of-view (FOV) tumor burden VOI containing all individual lesions was created. The lesion segmentation was verified and if necessary manually adjusted on SPECT and CT by two experienced readers in a consensus reading.

All VOIs were copied to the co-registered 48h and 72h SPECT images, and the activity values of each VOI were extracted to generate time-activity curves (TACs). TACs were fit to a mono-exponential

function using MATLAB (R2019b, The MathWorks, Inc. Natick, MA) to determine the effective half-lives ($T_{1/2\ eff}$) (*17*) for kidneys, individual lesions, and for the whole FOV tumor burden (TB_{FOV}). The procedure was performed for both therapy cycles.

Time-Integrated Activity with MTP and STP Approaches

The TIA for each VOI in the second therapy cycle was calculated using three different methods: 1) from the mono-exponential fit using all the points available from the MTP scans in the second cycle (considered the reference TIA (TIA_{ref}), determined from the activity at time t equals zero for the second therapy cycle, A_0^{2nd}, and $T_{1/2\ eff}$ for the second therapy cycle, $T_{1/2\ eff}^{2nd}$, see equation (1)), 2) by using $T_{1/2\ eff}$ determined from the curve fitting of the first cycle ($T_{1/2\ eff}^{1st}$, "prior information") and a STP activity value of the second cycle, and 3) using the approach suggested by Hänscheid.

$$TIA_{ref} = \frac{A_0^{2nd}}{ln2 / T_{1/2\ eff}^{2nd}} \quad (1)$$

Three different TIA_{STP} were calculated for the second method with equation (2) by combining $T_{1/2\ eff}^{1st}$ with the single activities A(t) measured at time t at 24h, 48h, or 72h. This approach is referred to as "STP_{prior}".

$$TIA_{STP_{prior}} = \frac{A(t) \cdot 2^{t / T_{1/2\ eff}^{1st}}}{ln2 / T_{1/2\ eff}^{1st}} \quad (2)$$

The third method estimated the TIA_{STP} using the method by Hänscheid. This approach assumes that if the imaging time point t is within 0.75 and 2.5 times $T_{1/2\ eff}$ of the respective VOI, one could replace equation (2) by the simplified formula (3) with less than 10% error in TIA compared to MTP. Three different TIA_{STP} were calculated using the activities A(t) measured at time t at 24h, 48h, or 72h. This approach is referred to as "STP_H".

$$TIA_{STP_H} \approx \frac{A(t)\cdot 2\cdot t}{ln2} \quad (3)$$

Comparisons

The STP approaches for the second therapy cycles were compared against the reference of MTP. The percentage difference (PD) in TIA_{STP} versus TIA_{ref} was calculated for each kidney, for the TB_{FOV}, and for up to six lesions per patient if they were visible in the FOV of both cycles. Bland-Altman plots were used to compare the STP approaches against MTP (*19,20*).

Statistical Analyses

Statistical analysis used the Wilcoxon signed-rank test between MTP and each of the respective STP approaches, and between $T_{1/2\ eff}$ of first and second cycles, respectively.

RESULTS

Unless otherwise stated, all reported values are given as average ± standard deviation [minimum; maximum].

Patients

Twenty patients with metastatic, castration-resistant prostate cancer were included in this analysis. The average administered activity of ^{177}Lu-PSMA-617 for all patients and therapy cycles was 6.09±0.13[5.74;6.70]GBq. Left and right kidneys were analyzed separately. The patients' volume of TB_{FOV} was on average 462±361[8;1229]ml. One patient had no lesions within the SPECT FOV. In total 56 lesions that were seen within the FOV of first and second therapy cycles were analyzed.

Distribution of Effective Half-Lives

Figures 2A, 2B, and 2C show the distribution of $T_{1/2\ eff}$ obtained with the MTP approach for the two therapy cycles for the kidneys, TB_{FOV}, and individual lesions, respectively. The average kidney $T_{1/2\ eff}$ were

32.5±7.0[17.8;51.9]h and 31.7±6.4[21.6;45.7]h for first and second therapy cycles, respectively. For TB_{FOV}, the average $T_{1/2\ eff}$ were 75.3±41.8[45.5;240.0]h and 64.8±35.0[14.5;192.8]h for first and second cycles, respectively. Average $T_{1/2\ eff}$ of 69.0±40.0[20.1;249.7]h and 66.6±34.2[19.7;216.2]h were found for first and second therapy cycles of the individual lesions. 26 of the 56 investigated lesions had a PD in $T_{1/2\ eff}$ of >±20%.

When comparing the $T_{1/2\ eff}$ obtained with MTP approaches from first and second therapy cycles using the Wilcoxon signed-rank test, significant statistical differences (i.e. $p<0.05$) were found for TB_{FOV} ($p=0.02$) (*N=19*; one patient had no lesions), while no significant statistical differences were found for the kidneys ($p=0.39$) (*N=37*; three patients had only one active kidney) and for the individual lesions ($p=0.27$) (*N=56*).

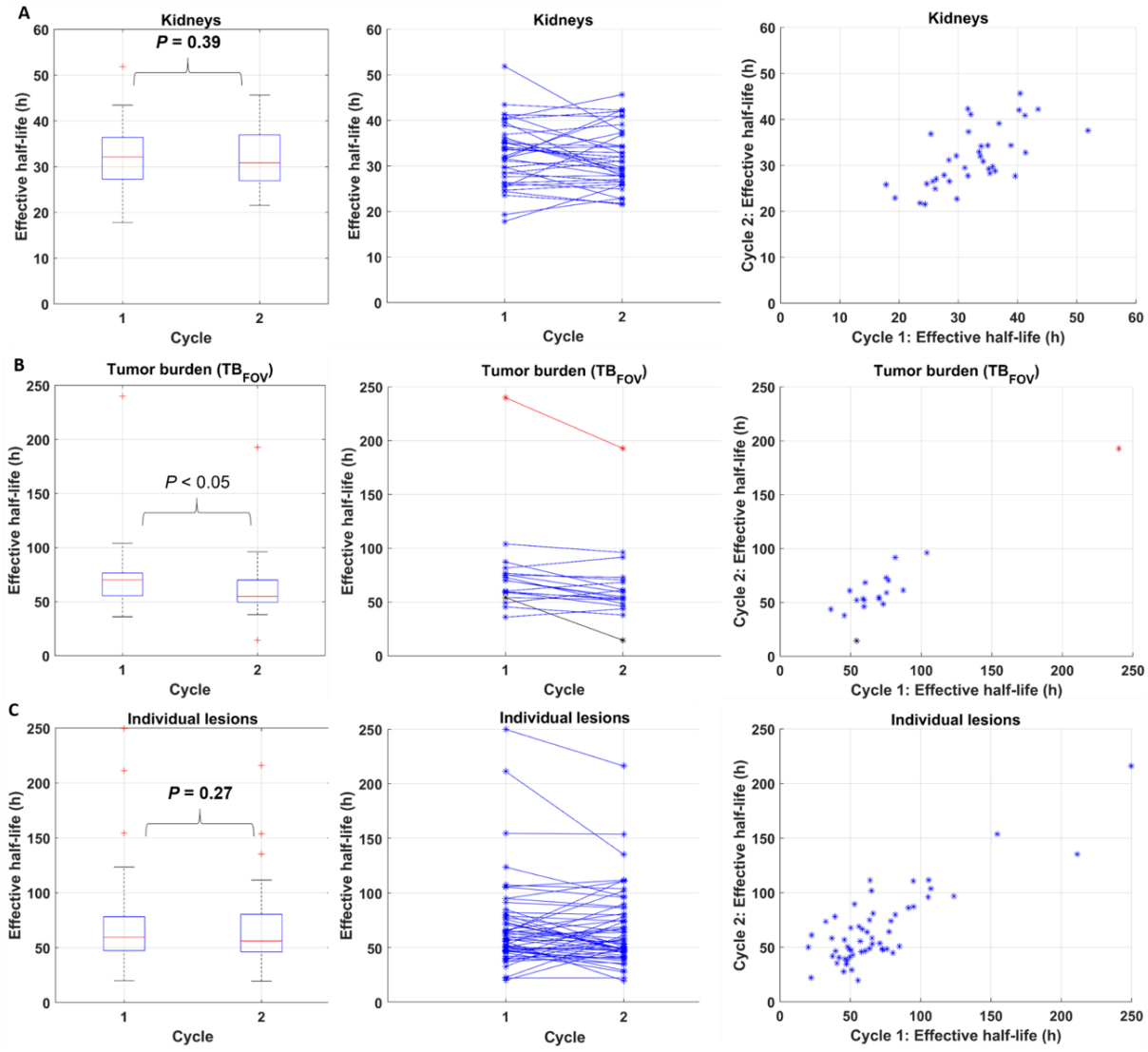

Figure 2: *Distribution of effective half-lives calculated using MTP methods for A) kidneys, B),* TB_{FOV}*, and C), individual lesions for both therapy cycles of* ^{177}*Lu-PSMA-617. The plots further include the results of the statistical analysis using the Wilcoxon signed-rank test for the* $T_{1/2\,eff}$ *between cycle 1 and cycle 2.*

Comparison of TIA with Respect to STP Approaches

Figure 3 shows the percentage differences in TIA between MTP and STP approaches. Supplementary Table 1 displays the tabulated values.

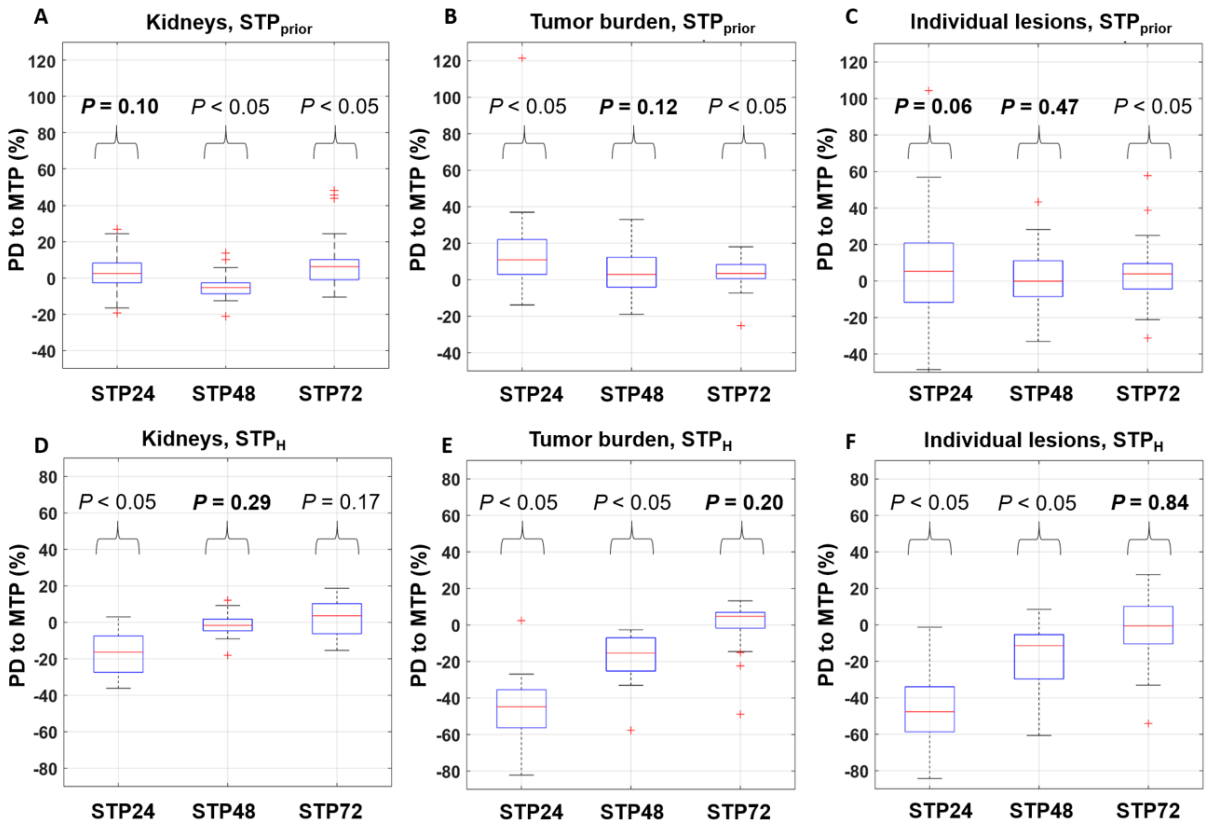

Figure 3: *Distribution of the PD of TIA in STP approaches relative to the reference MTP approach: for kidneys, tumor burden, and for individual lesions using* STP_{prior} *(A) and* STP_H *(B). The plots further include the results of the statistical analysis using the Wilcoxon signed-rank test between MTP and each of the respective STP approaches.*

The Bland-Altman plots of STP_{prior} and STP_H against MTP are given in Figures 4 and 5. The mean relative difference between MTP and STP_{prior} was closest to zero for the kidneys at 24h, for the TB_{FOV} at 72h, and for the individual lesions at 48h (Figure 4). However, the limits of agreement were smallest for the kidneys at 48h, for the TB_{FOV} at 72h, and for the individual lesions at 48h. For STP_H, the difference against MTP was closest to zero with smallest limits of agreement at 48h for kidneys and at 72h for individual lesions (Figure 5). For the TB_{FOV}, the difference was smallest at 72h, while the limits of agreements were slightly smaller at 48h.

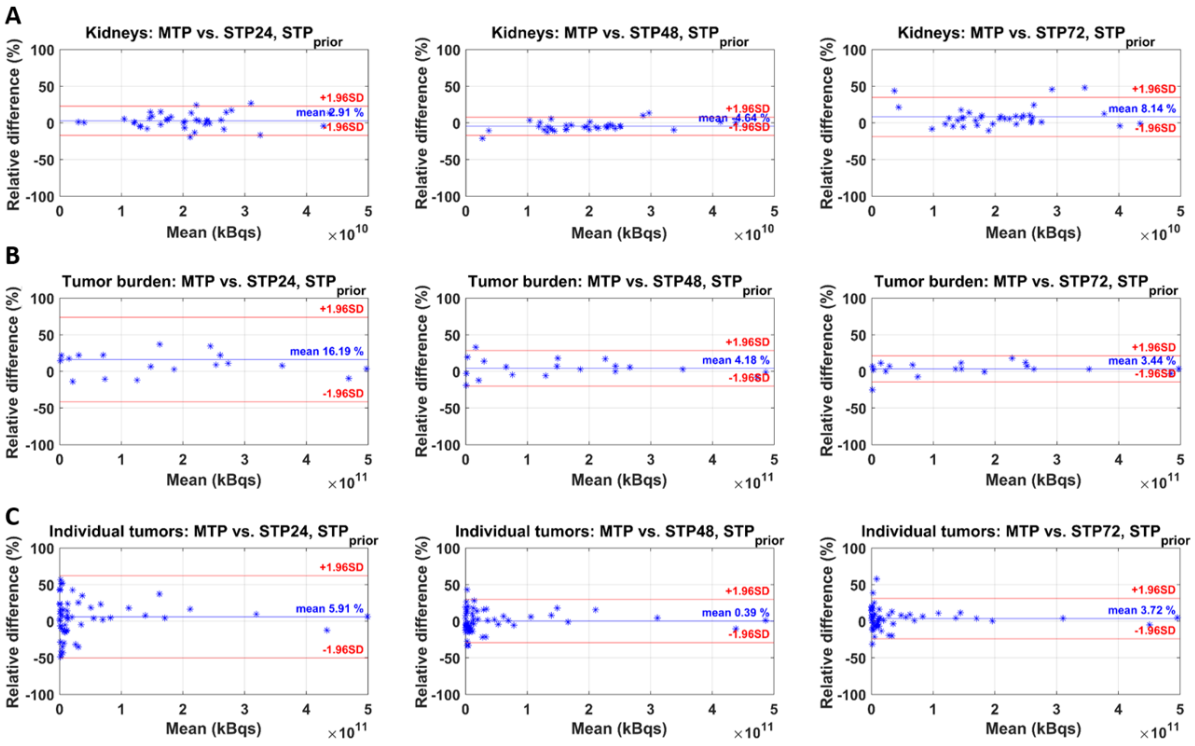

176

177 ***Figure 4:*** *Bland-Altman plots of the STP approaches against the reference of MTP for STP_{prior} for A) kidneys,*

178 *B) tumor burden, and C) individual lesions.*

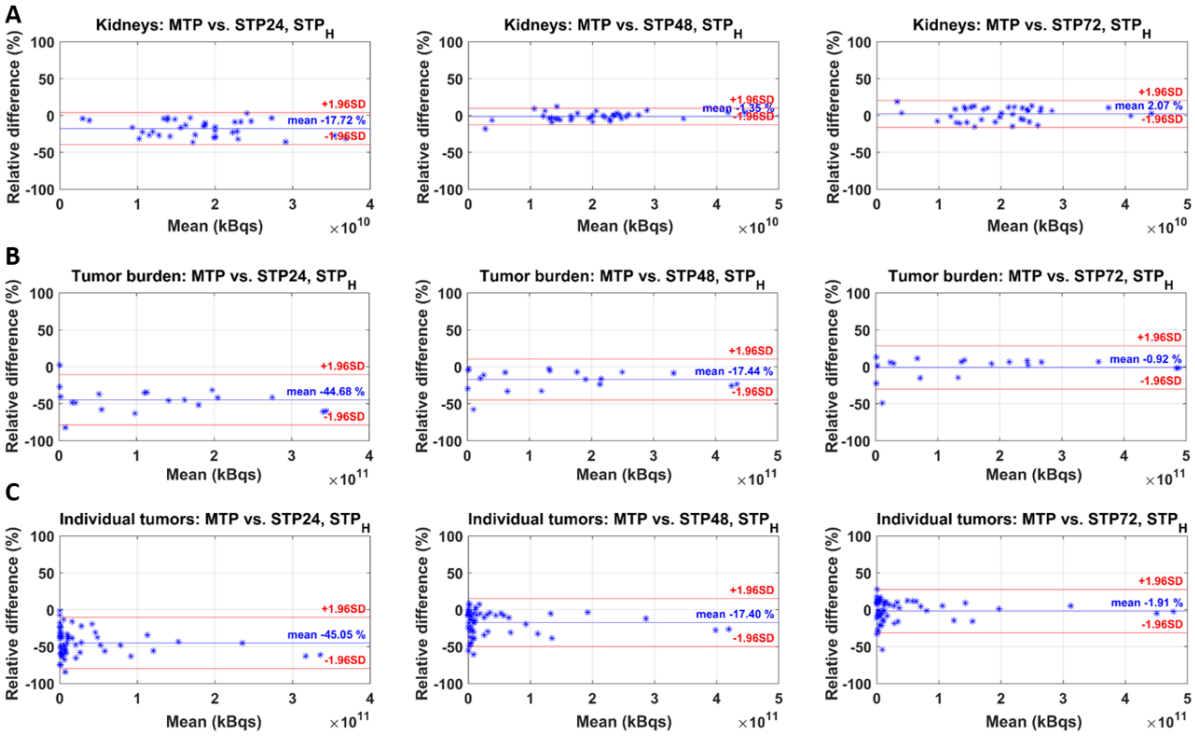

179

Figure 5: *Bland-Altman plots of the STP approaches against the reference of MTP for STP_H for A) kidneys, B) tumor burden, and C) individual lesions.*

Statistical Analyses

The results of the statistical analysis for the STP approaches against the reference of MTP are indicated in Figure 3. In general, no significant statistical difference in TIA for the kidneys was found for $STP_{prior}24$ and for STP_H48. For the TB_{FOV}, no significant statistical difference in TIA was found for $STP_{prior}48$ and for STP_H72. Lastly, for the individual lesions no significant statistical difference in TIA was found for $STP_{prior}24$ and $STP_{prior}48$ and STP_H72.

Table 1 summarizes the number and percentage of VOIs for which the imaging time points per therapy cycle were within 0.75 and 2.5 times $T_{1/2\ eff}$ of that region as calculated with a MTP approach. The imaging time point at 48h lied within $[0.75T_{1/2\ eff}, 2.5T_{1/2\ eff}]$ for 97% and 100% of the kidneys for both cycles 1 and 2, while for TB_{FOV} and individual lesions the largest number of VOIs within $[0.75T_{1/2\ eff}, 2.5T_{1/2\ eff}]$ was at 72h. However, for 25% of individual lesions and 21% of the TB_{FOV} VOIs, 72h was outside of the interval for cycle 2.

		# of VOIs with $t \in [0.75T_{1/2\,eff}, 2.5T_{1/2\,eff}]$		
		24h p.i.	48h p.i.	72h p.i.
Kidneys (*N=37*)	Cycle 1	7 (19%)	36 (97%)	28 (76%)
	Cycle 2	12 (32%)	37 (100%)	27 (73%)
TB_{FOV} (*N=19*)	Cycle 1	0 (0%)	6 (32%)	17 (89%)
	Cycle 2	1 (5%)	9 (47%)	15 (79%)
Individual lesions (*N = 56*)	Cycle 1	3 (5%)	26 (46%)	43 (77%)
	Cycle 2	2 (4%)	30 (54%)	42 (75%)

Table 1: *Number of VOIs for which the imaging time point (24h, 48h, or 72h p.i.) was within 0.75 and 2.5 times $T_{1/2\,eff}$ of either cycle 1 or cycle 2; the ratio against the total number is given in percent in brackets.*

Figure 6 shows the percentage of VOIs for which the TIA_{STP} is within ±10% and ±20% of TIA_{ref} for both the STP_{prior} and STP_H approaches. For STP_H, 95% of the kidneys were within ±10% of TIA_{ref} at 48h compared to 86% for STP_{prior}. For the TB_{FOV}, 95% of VOIs were within ±20% of TIA_{ref} at 48h and 72h for STP_{prior} compared to 68% and 89% for STP_H at 48h and 72h, respectively. For STP_{prior}, 86% and 91% of the individual lesions were within ±20% of TIA_{ref} at 48h and 72h, while is were 63% and 86% for STP_H at 48h and 72h, respectively.

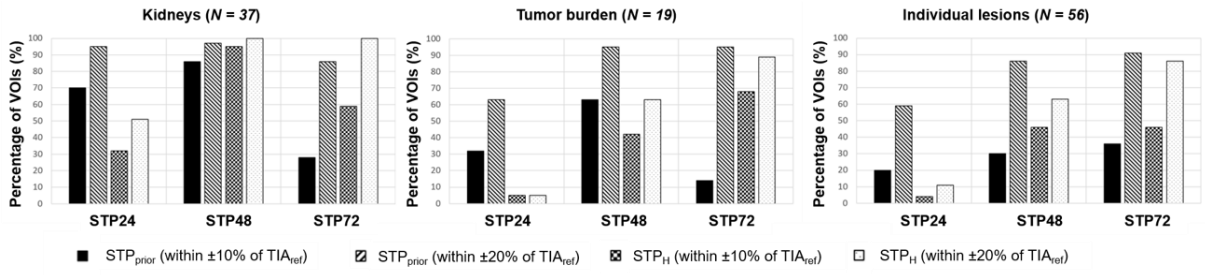

Figure 6: *Percentage of VOIs for which the difference in TIA for STP versus MTP falls within ±10% or ±20%.*

DISCUSSION

In this work, we aimed at comparing STP against MTP image-based dosimetry methods, which could increase adoption in the clinical environment. STP dosimetry methods have been studied predominantly for ^{177}Lu-DOTATATE therapy (*13,21-23*), but also for ^{177}Lu-PSMA therapy (*24-26*). Three different approaches for STP dosimetry have been proposed: 1) using population based mean $T_{1/2\ eff}$ (*27*), 2) using prior information from the first therapy cycle for subsequent cycles (*26*), and 3) using the formula by Hänscheid et al. (*13*). The first approach has been suggested to be valid for the calculation of kidneys ADs in ^{177}Lu-DOTATATE and ^{90}Y DOTATOC therapies (*22,27*). Given the mean $T_{1/2\ eff}$ of 32.5±7.0h and 31.7±6.4h of first and second ^{177}Lu-PSMA-617 therapy cycles determined from MTP imaging in this work, this approach could be a valid assumption. However, given the high variation and large spread of $T_{1/2\ eff}$ of TB_{FOV} and individual lesions in Figures 2B and 2C, the population based approach might not be suitable for lesion AD calculations in ^{177}Lu-PSMA therapies. Therefore, we compared clinically feasible dosimetry

approaches for kidneys and lesions with a reduced number of imaging time points based on method 2), the prior information approach STP_{prior}, and 3), the STP formula by Hänscheid STP_H.

STP based approaches showed smaller differences in TIA against TIA_{ref} for kidneys than for lesions. These differences can be associated with the smaller variations in $T_{1/2\ eff}$ (Figure 2). For the STP_{prior} approach, our analysis indicated that a STP at 24h p.i. results in TIA differences between STP24 and MTP that are on average closer to zero (Figure 3A, left). However, the 48h p.i. time point is more favorable if smaller range of variations in PD against TIA_{ref} are preferred (Figure 3A, left, and Figure 4A, middle). Our results agree with those reported by Kurth et al. (*26*) who applied the STP_{prior} approach for cycles 2 to 6, and found differences in AD of ±6% for kidneys and ±10% for parotid glands when using a single SPECT at 48h p.i. of ^{177}Lu-PSMA-617 compared to MTP. Our analysis also suggests that when using the STP_H approach, either a STP at 48h or 72h p.i. are favorable. However, a STP_H at 48h p.i. might be optimal for kidney AD calculations given the smaller range of variations of TIA_{STP} against TIA_{ref} (Figure 3B, left, and Figure 5A, middle). For the kidneys, STP_H outperformed STP_{prior} at 48h in terms of PD in TIA with respect to MTP (Figure 6). With $STP_{H,}$ the great majority (95%) of kidney TIAs are expected to be within 10% of those calculated with MTP with few (5%) of them falling within 10%-20%. For kidneys, the 48h imaging time point is within the $[0.75T_{1/2\ eff}, 2.5T_{1/2\ eff}]$ interval for all kidneys except for one. STP_H therefore yielded TIA estimates very close to TIA_{ref}. STP_{prior} on the other hand relies on comparable $T_{1/2\ eff}$ of cycle 1 and 2. We observed up to 45% difference in $T_{1/2\ eff}$ for some of the investigated kidneys. However, this did translated only in a PD to TIA_{ref} between -6% and 14%, which could be tolerated as long as the overall kidney function of the patient prior to therapy was good and the cumulative kidney absorbed dose is far below the considered toxicity threshold of 23Gy.

For the TB_{FOV} and individual lesions, an imaging time point at 72h p.i. seems to be optimal as the ranges of PD against MTP are the smallest (Figure 3A, middle, right, and Figures 4B,C, right) for the STP_{prior} approach. Similar for STP_H, the PD against MTP was closer to zero at 72h p.i. (Figure 3B, middle, right, and

242 Figures 5B,C, right). However, to obtain TIA estimates for both, kidneys and lesions, in a single scan, a STP
243 at 48h p.i. could be a valid compromise. But this compromise comes at a higher variation in PD with respect
244 to MTP for the lesions.

245 With respect to Figure 6, STP_{prior} overall performed better for TB_{FOV} and individual lesions than
246 STP_H. The performance of STP_H improved with later imaging time points. This agrees with findings reported
247 by Hänscheid et al. (*13*) for ^{177}Lu-DOTATATE and Jackson et al. (*25*) for ^{177}Lu-PSMA-617; both revealing
248 better agreement of STP with MTP for lesions at imaging time points even beyond 72h. STP_H showed
249 overall an underestimation of TIA for TB_{FOV} and individual lesions in Figure 3B. Similar observations of a
250 negative skew for STP_H were previously reported by Gustafsson et al. (*28*). This underlines, that the
251 application of STP approaches is limited by their accuracy and the distribution of $T_{1/2\ eff}$ in a population
252 must be carefully determined. Our results however, suggest that STP_{prior} is more suitable for tumor
253 dosimetry especially if the time point should be 48h, matching our recommendation for the kidneys. For
254 STP_{prior}, it is expected that the majority of the TIAs fall within 20% of the ones calculated with MTP. Our
255 suggestion to perform SPECT imaging at 48h p.i. is in agreement with the analysis performed by Hou et al.
256 (*24*). Generally, this recommendation is limited for STP_H since with respect to Table 1, the imaging time
257 point of 48h is outside of the $[0.75T_{1/2\ eff}, 2.5T_{1/2\ eff}]$ interval for about 50% of the individual lesions for cycles
258 1 and 2 and for 50-60% of the TB_{FOV}.

259 The hybrid MTP/STP (STP_{prior}) approach presented here allows for the collection of all the required
260 SPECT images during the routine three day hospital stay for patients receiving ^{177}Lu-PSMA-617 therapy at
261 our institution. This data collection should, however, still be feasible for other institutions with in-patient
262 therapies but also for centers that discharge the patients on day 0 if the patients comply with coming back
263 during the following 2 days. We understand that the latter situation is not optimal but open
264 communication with the patient highlighting the benefit of MTP imaging during first therapy cycle could
265 increase the patient's willingness to cooperate and participate in multiple scans. In cases where a patient

could only tolerate STP imaging (e.g. due to pain) or where only one scan is feasible due to scanner availability or reimbursement issues, the STP_H approach could still be valid but imaging should be performed at 72h p.i. or later (Figure 6), for which we observed differences in TIA to be within ±20% for all kidneys and for over 85% of the investigated TB_{FOV} and individual lesions. In our investigation, this would ensure that the imaging time point is within the $[0.75T_{1/2\,eff}, 2.5T_{1/2\,eff}]$ interval for over 70% of the kidneys, TB_{FOV} and individual lesions as shown in Table 1.

Specific patient situations should be considered when applying STP methods. The STP_{prior} approach might be more prone to deviations against TIA_{ref} for lesions in cases of progressive disease or fast response (Supplementary Figure 1). The protection of healthy organs from radiation-induced toxicities trumps achieving highest possible lesion doses. When considering the minimum and maximum PDs of -21% and 14% for kidney TIA achieved with STP_{prior} at 48h p.i. and -18.1% to 12.1% with STP_H, this bears the risk to under- or overestimate the actual kidney dose. Dose underestimation in the individual patient could lead to the application of subsequent therapy cycles although the kidney dose threshold was already exceeded. ADs obtained from STP methods should therefore be interpreted with caution with respect to approximately 20% underestimation in a few patients. Patient-individual condition and kidney function prior to therapy and during the course of treatment must be closely monitored to prevent from radiation-induced toxicity. Our analysis revealed large minimum and maximum PDs of -19% to 33% for TB_{FOV} and -33% to 43% for individual lesions for STP_{prior} at 48h p.i., and -58% to -3% for TB_{FOV} and -61% to 8% for individual lesions when using STP_H. Since current clinical practise focuses on the protection of healthy organs, this will likely not influence the patient's course of treatment. However, this variation in lesion AD with possible over- and underestimation of the actual lesion AD can potentially impact the derivation of dose-response relationships for prostate cancer lesions. The research community should therefore focus on MTP-derived lesion ADs to determine the response of lesions to ^{177}Lu-PSMA-617 therapy of prostate cancer. In case the therapeutic scheme for PSMA therapy includes PET/CT staging after every second

therapy cycle, this could be used to guide whether MTP imaging might become necessary for the subsequent therapy cycle due to large changes in tumor burden.

We recognize the limitation that our imaging protocol did not include time points after 72h p.i. This study was based on the available imaging data at our institution that was acquired during the routine three day hospital stay of the patients receiving ^{177}Lu-PSMA-617 therapy. However, our collected imaging time points are aligned with other institutions at least in a comparable temporal range (*26,29-31*). Further research should be performed to assess the validity of our results including time points at 96h p.i. or later. This could potentially lead to a different favorable time point of the STP approach for lesions due to their longer retention time (*32*) than was shown in our study. The herein suggested imaging time point of 48h p.i. ensured that the TIA determined with STP_{prior} is within ±20% of TIA_{ref} for 97% of the investigated kidneys, 95% of the TB_{FOV}, and 86% of the individual lesions (Figure 6). However, the 48h time point is outside of the $[0.75T_{1/2\ eff}, 2.5T_{1/2\ eff}]$ interval for about 50% of the individual lesions for cycles 1 and 2 and for 50-60% of the TB_{FOV} (Table 1). An imaging time point at 72h might be more applicable for STP_H for lesions but with larger differences from TIA_{ref} for the kidneys.

Patients with mCRPC can present with a large amount of metastases, which could challenge to track the lesions across cycles and to calculate absorbed dose values on an individual lesion basis. Our analysis for individual lesions was therefore limited to six representative lesions per patient. Organ and lesion $T_{1/2\ eff}$ may not only depend on the individual patient but can vary to a large extend between radiopharmaceuticals, compare with Table 2 of Hou et al. (*24*) and Figure 3 of Schuchardt et al. (*33*). The applicability of different STP dosimetry approaches should therefore be carefully investigated for different organs, tumors and different radiopharmaceuticals. Future work should include organs that were outside or not entirely within the FOV of our 1-bed SPECT and all lesions per patient as well as expanding the analysis to other PSMA compounds. Further studies could be directed to investigate how parameters that can be acquired prior to therapy can impact $T_{1/2\ eff}$. MTP imaging might be advisable in case certain

parameters such as for example the eGFR are out of the normal range to precisely capture patient-individual $T_{1/2\ eff}$. On the other hand, it can be assessed whether STP approaches are still valid but at different favorable imaging time points. Nevertheless, our results suggest that STP dosimetry is feasible for ^{177}Lu-PSMA-617 therapies. We hope that these findings, that simplify dosimetry clinical workflows, ease implementation of routine dosimetry in RPTs.

CONCLUSION

The present study assessed STP image-based dosimetry of ^{177}Lu-PSMA-617 therapy of prostate cancer. The approaches using a single SPECT/CT at 48h or 72h post administration of the radiopharmaceutical led to differences against the MTP based dosimetry that were overall within ±20%. Both, full STP dosimetry using the Hänscheid formula as well as the prior information STP approach based on effective half-lives from MTP imaging of the first cycle demonstrated their validity for ^{177}Lu-PSMA-617. Since STP based dosimetry reduces the burden for patients and the overall costs and complexity of dosimetry, it facilitates the implementation of dosimetry into routine clinical practice of radiopharmaceutical therapies.

Disclosure

The authors declare that they have no conflict of interest. This work was partly funded by the German Research Foundation (DFG) within the Research Training Group GRK2274 (Julia Brosch-Lenz).

Key Points

Question: Can the number of imaging time points required for dosimetry be reduced?

Pertinent Findings: STP dosimetry is feasible using either the simplified formula by Hänscheid or a prior information approach that uses MTP imaging for the first therapy cycle with STP imaging for subsequent therapy cycles. Both methods allow for patient-individual dosimetry of kidneys and lesions with less than ±20% difference from MTP based approaches.

Implications for patient care: Patient will benefit from personalized dosimetry and related risk and outcome prediction.

REFERENCES

1. Sartor O, de Bono J, Chi KN, et al. Lutetium-177-PSMA-617 for metastatic castration-resistant prostate cancer. *N Engl J Med*. 2021;385:1091-103.

2. Hofman MS, Violet J, Hicks RJ, et al. [(177)Lu]-PSMA-617 radionuclide treatment in patients with metastatic castration-resistant prostate cancer (LuPSMA trial): a single-centre, single-arm, phase 2 study. *Lancet Oncol*. 2018;19:825-33.

3. Baum RP, Kulkarni HR, Schuchardt C, et al. 177Lu-labeled prostate-specific membrane antigen radioligand therapy of metastatic castration-resistant prostate cancer: safety and efficacy. *J Nucl Med*. 2016;57:1006-13.

4. Ahmadzadehfar H, Rahbar K, Kürpig S, et al. Early side effects and first results of radioligand therapy with (177)Lu-DKFZ-617 PSMA of castrate-resistant metastatic prostate cancer: a two-centre study. *EJNMMI Res*. 2015;5:114.

5. Delker A, Fendler WP, Kratochwil C, et al. Dosimetry for (177)Lu-DKFZ-PSMA-617: a new radiopharmaceutical for the treatment of metastatic prostate cancer. *Eur J Nucl Med Mol Imaging*. 2016;43:42-51.

6. Garin E, Tselikas L, Guiu B, et al. Personalised versus standard dosimetry approach of selective internal radiation therapy in patients with locally advanced hepatocellular carcinoma (DOSISPHERE-01): a randomised, multicentre, open-label phase 2 trial. *Lancet Gastroenterol Hepatol*. 2021;6:17-29.

7. Kratochwil C, Fendler WP, Eiber M, et al. EANM procedure guidelines for radionuclide therapy with (177)Lu-labelled PSMA-ligands ((177)Lu-PSMA-RLT). *Eur J Nucl Med Mol Imaging*. 2019;46:2536-44.

8. Brosch-Lenz J, Yousefirizi F, Zukotynski K, et al. Role of artificial intelligence in theranostics: Toward routine personalized radiopharmaceutical therapies. *PET Clin*. 2021;16:627-41.

9. Strigari L, Konijnenberg M, Chiesa C, et al. The evidence base for the use of internal dosimetry in the clinical practice of molecular radiotherapy. *Eur J Nucl Med Mol Imaging*. 2014;41:1976-88.

10. Violet J, Jackson P, Ferdinandus J, et al. Dosimetry of (177)Lu-PSMA-617 in metastatic castration-resistant prostate cancer: Correlations between pretherapeutic imaging and whole-body tumor dosimetry with treatment outcomes. *J Nucl Med*. 2019;60:517-23.

11. Graves SA, Bageac A, Crowley JR, Merlino DAM. Reimbursement approaches for radiopharmaceutical dosimetry: Current status and future opportunities. *J Nucl Med*. 2021;62(Suppl 3):48s-59s.

12. European Commission. Council Directive 2013/59/Euratom of 5 December 2013 laying down basic safety standards for protection against the dangers arising from exposure to ionising radiation, and repealing Directives 89/618/Euratom, 90/641/Euratom, 96/29/Euratom, 97/43/Euratom and 2003/122/Euratom. *Official Journal of the European Union*. 2014.

13. Hänscheid H, Lapa C, Buck AK, Lassmann M, Werner RA. Dose mapping after endoradiotherapy with (177)Lu-DOTATATE/DOTATOC by a single measurement after 4 days. *J Nucl Med*. 2018;59:75-81.

14. Ljungberg M, Celler A, Konijnenberg MW, et al. MIRD pamphlet No. 26: Joint EANM/MIRD guidelines for quantitative 177Lu SPECT applied for dosimetry of radiopharmaceutical therapy. *J Nucl Med*. 2016;57:151-62.

15. Uribe CF, Esquinas PL, Tanguay J, et al. Accuracy of (177)Lu activity quantification in SPECT imaging: a phantom study. *EJNMMI Phys*. 2017;4:2.

16. Gosewisch A, Delker A, Tattenberg S, et al. Patient-specific image-based bone marrow dosimetry in Lu-177-[DOTA(0),Tyr(3)]-Octreotate and Lu-177-DKFZ-PSMA-617 therapy: investigation of a new hybrid image approach. *EJNMMI Res*. 2018;8:76.

17. Brosch-Lenz J, Uribe C, Gosewisch A, et al. Influence of dosimetry method on bone lesion absorbed dose estimates in PSMA therapy: application to mCRPC patients receiving Lu-177-PSMA-I&T. *EJNMMI Phys*. 2021;8:26.

18. Gafita A, Bieth M, Krönke M, et al. qPSMA: Semiautomatic software for whole-body tumor burden assessment in prostate cancer using (68)Ga-PSMA11 PET/CT. *J Nucl Med*. 2019;60:1277-83.

19. Bland JM, Altman DG. Statistical methods for assessing agreement between two methods of clinical measurement. *Lancet*. 1986;1:307-10.

20. Bland JM, Altman DG. Measuring agreement in method comparison studies. *Stat Methods Med Res*. 1999;8:135-60.

21. Del Prete M, Arsenault F, Saighi N, et al. Accuracy and reproducibility of simplified QSPECT dosimetry for personalized (177)Lu-octreotate PRRT. *EJNMMI Phys*. 2018;5:25.

22. Zhao W, Esquinas PL, Frezza A, Hou X, Beauregard JM, Celler A. Accuracy of kidney dosimetry performed using simplified time activity curve modelling methods: a (177)Lu-DOTATATE patient study. *Phys Med Biol*. 2019;64:175006.

23. Willowson KP, Eslick E, Ryu H, Poon A, Bernard EJ, Bailey DL. Feasibility and accuracy of single time point imaging for renal dosimetry following (177)Lu-DOTATATE ('Lutate') therapy. *EJNMMI Phys*. 2018;5:33.

24. Hou X, Brosch J, Uribe C, et al. Feasibility of single-time-point dosimetry for radiopharmaceutical therapies. *J Nucl Med*. 2021;62:1006-11.

25. Jackson PA, Hofman MS, Hicks RJ, Scalzo M, Violet J. Radiation dosimetry in (177)Lu-PSMA-617 therapy using a single posttreatment SPECT/CT scan: A novel methodology to generate time- and tissue-specific dose factors. *J Nucl Med*. 2020;61:1030-6.

26. Kurth J, Heuschkel M, Tonn A, et al. Streamlined schemes for dosimetry of (177)Lu-labeled PSMA targeting radioligands in therapy of prostate cancer. *Cancers (Basel)*. 2021;13:3884.

27. Madsen MT, Menda Y, O'Dorisio TM, O'Dorisio MS. Technical note: Single time point dose estimate for exponential clearance. *Med Phys*. 2018;45:2318-24.

28. Gustafsson J, Taprogge J. Theoretical aspects on the use of single-time-point dosimetry for radionuclide therapy. *Phys Med Biol*. 2022;67(2).

29. Hohberg M, Eschner W, Schmidt M, et al. Lacrimal glands may represent organs at risk for radionuclide therapy of prostate cancer with [(177)Lu]DKFZ-PSMA-617. *Mol Imaging Biol*. 2016;18:437-45.

30. Peters SMB, Privé BM, de Bakker M, et al. Intra-therapeutic dosimetry of [(177)Lu]Lu-PSMA-617 in low-volume hormone-sensitive metastatic prostate cancer patients and correlation with treatment outcome. *Eur J Nucl Med Mol Imaging*. 2022;49:460-9.

31. Privé BM, Peters SMB, Muselaers CHJ, et al. Lutetium-177-PSMA-617 in low-volume hormone-sensitive metastatic prostate cancer: A prospective pilot study. *Clin Cancer Res*. 2021;27:3595-601.

32. Rinscheid A, Kletting P, Eiber M, Beer AJ, Glatting G. Influence of sampling schedules on [(177)Lu]Lu-PSMA dosimetry. *EJNMMI Phys*. 2020;7:41.

33. Schuchardt C, Zhang J, Kulkarni HR, Chen X, Müller D, Baum RP. Prostate-specific membrane antigen radioligand therapy using (177)Lu-PSMA I&T and (177)Lu-PSMA-617 in patients with metastatic castration-resistant prostate cancer: Comparison of safety, biodistribution, and dosimetry. *J Nucl Med*. 2022;63:1199-207.

SUPPLEMENTARY DATA

MATERIAL AND METHODS

Imaging protocol

Imaging followed our institutions' routine clinical imaging protocol for dosimetry (Figure 1). Patients underwent MTP quantitative ^{177}Lu-SPECT/CT imaging during their three day hospital stay at approximately 24h, 48h, and 72h post injection (p.i.) of ^{177}Lu-PSMA-617. SPECT acquisition was performed with one bed position covering the abdominal region on a dual-head Symbia T2 SPECT/CT (Siemens Healthcare, Germany) equipped with a medium-energy low-penetration collimator and using three energy windows: 208keV (15% width, upper photo peak of ^{177}Lu), 170keV (15% width, lower scatter window), and 240keV (10% width, upper scatter window) (*5,14,15*). A low dose CT was acquired during the first image acquisition session for attenuation correction (AC). The quantitative image reconstruction (20 MAP iterations, 16 subsets, Bayesian weight 0.001 (*16*) included triple-energy window scatter correction, AC, and the distance-dependent geometrical collimator modelling as described by Delker et al. (*5*). AC of the 48h and 72h SPECT scans was performed using the 24h CT which was co-registered to an initial non-attenuation corrected SPECT reconstruction of these time points (*17*). A system-specific calibration factor was applied to generate images in units of activity concentration (Bq/ml) (*18*).

RESULTS

The values from Figure 3 are provided in supplementary Table 1.

Supplementary Table 1: Percentage difference in TIA against MTP. Values are given in average ± standard deviation [minimum, maximum] [%].

	STP_{prior} vs MTP			STP_H vs MTP		
	STP24	STP48	STP72	STP24	STP48	STP72
Kidneys (n=37)	2.9 ±10.0 [-19.2, 26.7]	-4.6 ± 6.2 [-21.0, 13.6]	8.1 ± 13.4 [-10.5, 48.1]	-17.7 ±10.9 [-36.2; 3.0]	-1.3 ± 5.6 [-18.1; 12.1]	2.1 ± 9.2 [-15.2; 18.7]
TB_{FOV} (n=19)	16.2 ± 28.7 [-13.8, 121.4]	4.2 ± 12.1 [-19.0, 33.0]	3.4 ± 8.9 [-25.2, 18.0]	-44.7 ± 17.0 [-82.3; 2.4]	-17.4 ± 13.7 [-57.7; -2.7]	-0.9 ± 14.6 [-49.0; 13.2]
Individual lesions (n=56)	5.9 ± 28.4 [-48.5, 104.3]	0.4 ± 14.9 [-33.1, 43.2]	3.7 ± 14.0 [-31.2, 57.7]	-45.0 ± 17.6 [-84.3; -1.3]	-17.4 ± 16.4 [-60.7; 8.5]	-1.9 ± 14.8 [-54.1; 27.5]

The two patients with largest percentage deviations (>>±20%) of STP_{prior} against MTP for the TB_{FOV} are shown in supplementary Figure 1. Both patients showed either a large reduction in tumor burden between first and second therapy cycle, or presented with small lymphatic lesions that were challenging to segment. This resulted in the largest deviations in Figures 2B,C for TB_{FOV} and individual lesions when the STP_{prior} approach was used. The patient in supplementary Figure 1A corresponds to the black line in Figure 2B, while the patient in supplementary Figure 1B corresponds to the red line in Figure 2B.

Here, the differences of the effective half-lives between first and second therapy cycle (compare with red and black line in Figure 2B), influenced the pharmacokinetics of the later cycle. Removing these patients from the STP_{prior} analysis would reduce the PD in TIA from STP48 against TIA_{ref} from 4.2±12.1[-19.0;33.0]% to 3.8±9.1[-12.3;19.5]% for TB_{FOV} and from 0.4±14.9[-33.1;43.2]% to -0.7±13.5[-33.1;26.4]%.

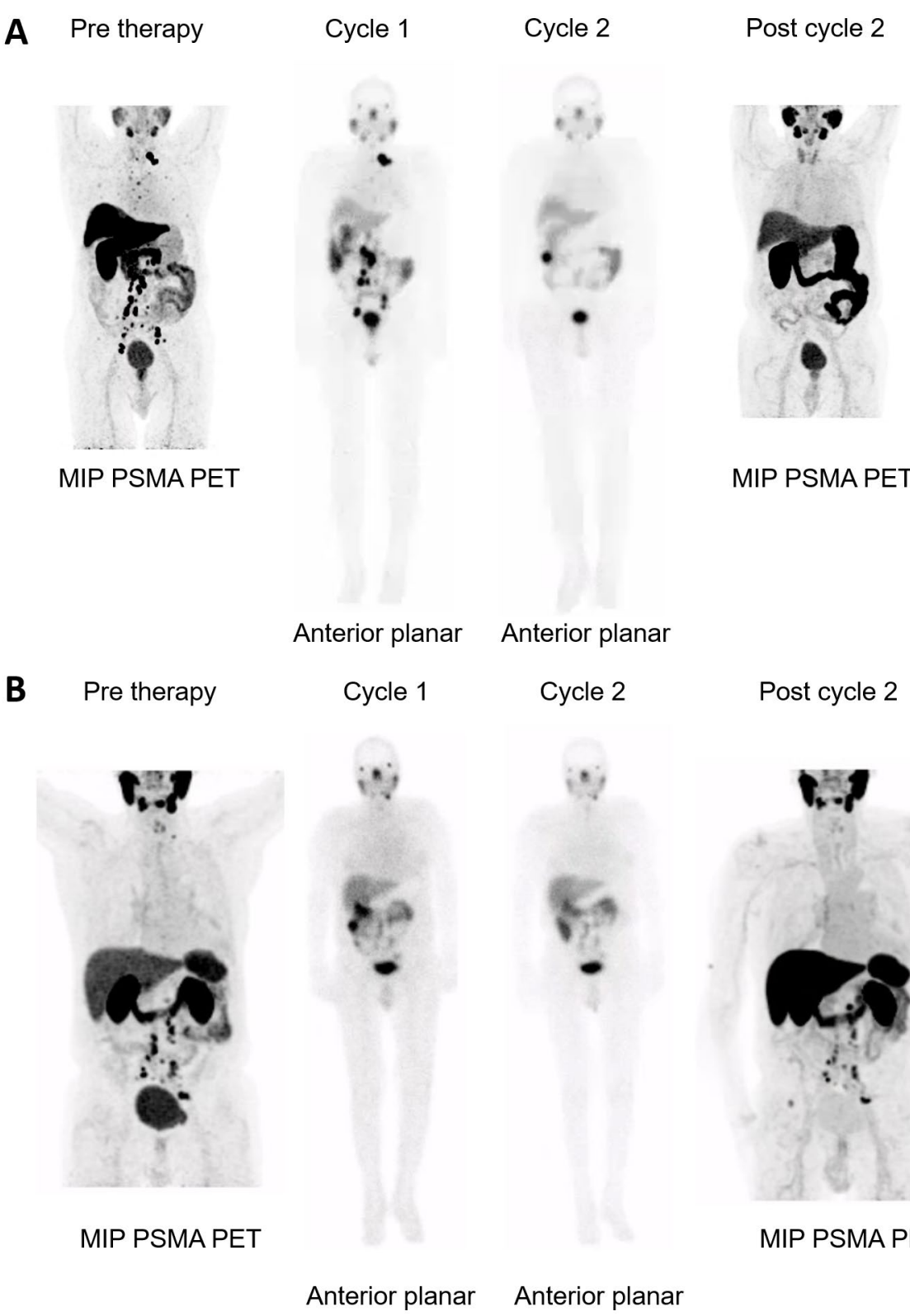
A
Pre therapy
Cycle 1
Cycle 2
Post cycle 2
MIP PSMA PET
Anterior planar
Anterior planar
MIP PSMA PET
B
Pre therapy
Cycle 1
Cycle 2
Post cycle 2
MIP PSMA PET
Anterior planar
Anterior planar
MIP PSMA PET

Supplemental Figure 1: *Maximum intensity projections (MIP) of the pre- and post-cycle 2 therapy PSMA PETs and the anterior views of the planar ^{177}Lu-PSMA image of the first and second therapy cycle of the two patients with largest deviations of the STP_{prior} against the MTP approach for TTB_{FOV}. For patient A), the first therapy cycle took place two weeks after the first PET, and the second PET took place two months after the second therapy cycle. For patient B), the first therapy cycle took place one week after the first PET and the second PET took place 3 months after the second therapy cycle. For illustration purposes, the planar whole-body scans are displayed.*